PANCHAKOTesSAYS
ISSN : 0976-4968
Vol-15, No.-2, November 2024

Development of Concerted Metalation Deprotonation (CMD) Mechanism

S. M. Wahidur Rahaman

Assistant Professor, Dept. of Chemistry, Panchakot Mahavidyalaya, Sarbari, P.O. Neturia, Dist. Purulia, Pin: 723121, West Bengal, India. Email:*wrahaman@gmail.com*

Abstract

The process of C-H bond activation is crucial for catalytic events. There are several known ways for activating C-H bonds. For the activation of C-H bonds, one of the key pathways is Concerted Metalation Deprotonation (CMD). The application of CMD in the field of C-H functionalization has been widespread. The development of the CMD mechanism was appropriately covered in this short review from the very beginning. Selected mechanistic studies of this reaction will be discussed. The ligand on the metal center is important role in this transformation.

KEYWORDS: C-H Bond Activation, Concerted Metalation Deprotonation, Metal Complex, Computational Study, Base Assisted.

INTRODUCTION

The reaction of C-H functionalization is crucial for the synthesis of organic compounds[1]. C-H functionalization can be studied via a various of mechanisms, including oxidative addition, electrophilic pathway, sigma-bond metathesis, and others[2]. In electrophilic C-H bond activation, one of the key mechanisms is concerted metalation deprotonation (CMD). CMD has been investigated conceptually and experimentally and is a well-established process in the literature[3]. A base, such as acetate, and carbonate always helps the CMD process. In this paper the evolution of CMD chemistry was explained right away. This process was discussed experimentally and computationally using different metal complexes from published papers.

EARLIER EVIDENCE OF C-H BOND ACTIVATION

Otto Dimroth observed in 1902 that benzene and mercury acetate react to generate phenylmercuric acetate at a temperature of 110–120°C (Scheme 1)[4].

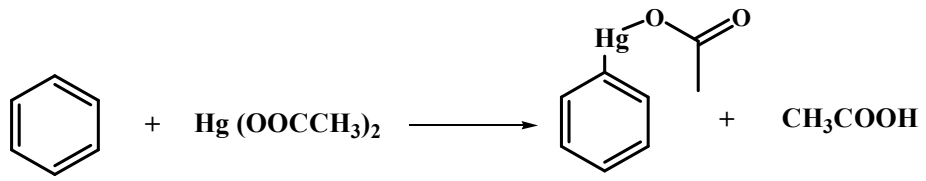

Scheme 1: Formation of phenylmercuric acetate

When Winstein and Traylor[5] initially talked about CMD in 1955, they reported that RH and RHgOAc compounds were synthesized from R_2Hg (where R = phenyl, s-butyl, and n-butyl) using an electrophilic substitution pathway (Scheme 2).

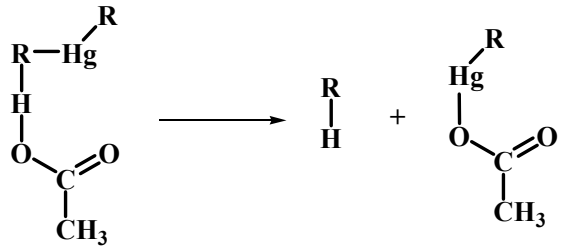

R = phenyl, s-butyl, n-butyl

Scheme 2: Proton transfer from acetic acid to alkyl or aryl group

The arene mercurinium ions (Scheme 3), which are intermediate complexes of aromatic mercuriation as demonstrated by proton and carbon-13 NMR studies, were presented to George A. Olah[6].

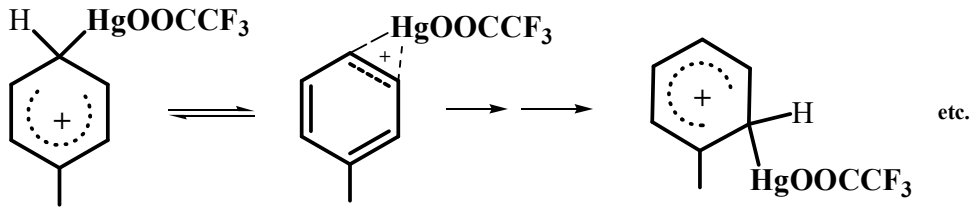

Scheme 3: Formation of arenemercurinium ions

CYCLOMETALLATED COMPOUND

Cope and Siekman[7] talked about forming new covalent bonds between metal and carbon by a direct substitution reaction in an article. Aromatic azo compounds and potassium tetrachloro- platinate (II) or palladium (II) dichloride have been found to

react unusually, producing cyclometallated platinum (II) and palladium (II) compounds (Scheme 4).

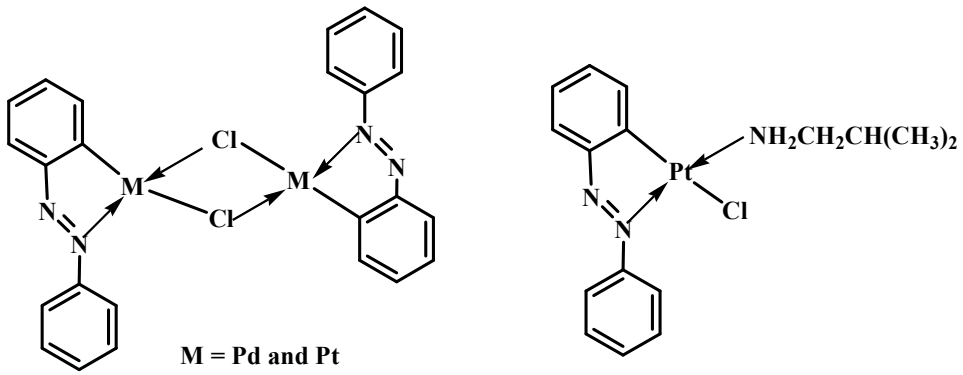

Scheme 4: Formation of new bond between metal and carbon

Cope and Friedrich[8] simultaneously demonstrated how platinum (II) and palladium (II) chlorides react with N, N-dimethylbenzylamines to form carbon-to-metal linked platinum (II) and palladium (II) complexes via an electrophilic aromatic substitution process (Scheme 5).

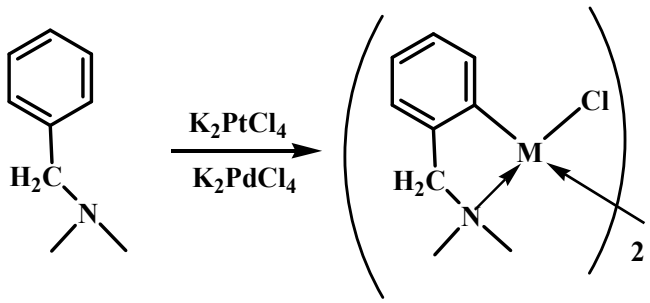

Scheme 5: Formation of new bond between Pd(II)/Pt(II) and carbon

Using an electrophilic pathway, J. M. Davidson[9] initially demonstrated how diacetate palladium reacts with aromatic hydrocarbons to form biphenyl compounds (Equation 1).

$$2C_6H_6 + Pd(OAc)_2 = Pd\ (0) + (C_6H_5)_2 + 2HOAc$$

Equation 1: Biphenyl compound from the reaction of benzene and $Pd(OAc)_2$ throgh electrophilic path way

The ortho-palladation of ring-substituted N, N-dimethylbenzylamines was reported by Ryabov and Yatsimirsky[10]. They examine the mechanism and kinetics

(Scheme 6), and they suggest that acetate causes proton abstraction in the transition state structure, whereas external amine does not (Figure 1).

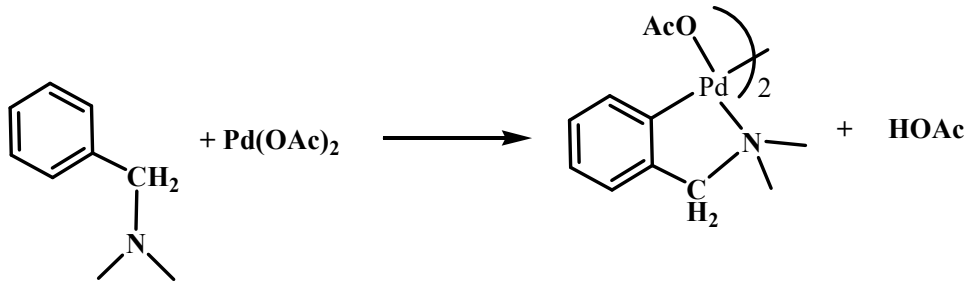

Scheme 6: Ortho-palladation of N,N-dimethylbenzylamine ligand

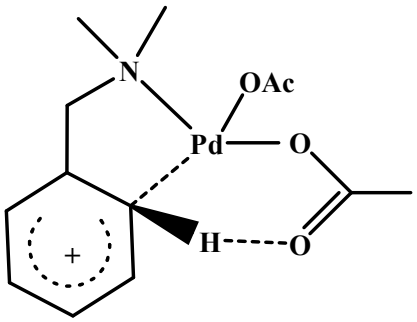

Figure 1: Proposed transition state of proton abstraction by acetate

THEORETICAL STUDY OF C-H BOND ACTIVATION

Sakaki[11] conducted a theoretical investigation of $M(\eta^2\text{-}O_2CH)_2$ (M = Pd or Pt) activating C-H bonds in benzene and methane using DFT computation (Scheme 7). The benzene and palladium formate complex exhibit van der Waals attraction, forming the first intermediate **2a**. After that, it passes through **TS 2a-3a**, the transition stage, and emerges as intermediate **3a**. With a activation energy of 3.8 kcal/mol, one oxygen atom separates from the metal in a transition state structure. The following phase involves oxygen abstracting the proton from the aromatic benzene through a six-membered transition state **TS 3a-4a**. The activation barrier in this case is 16.1 kcal/mol, and product **4a** is the result. The activation barrier for platinum metal, which was also investigated using this process, is 21.2 kcal/mol.

Energy activation values for palladium and platinum were determined to be 21.5 and 17.3 kcal/mol, respectively, when the same mechanism was investigated for methane via $M(\eta^2\text{-}O_2CH)_2$ (M = Pd, Pt). Based on this data, it was determined that C-H activation occurs readily under these circumstances.

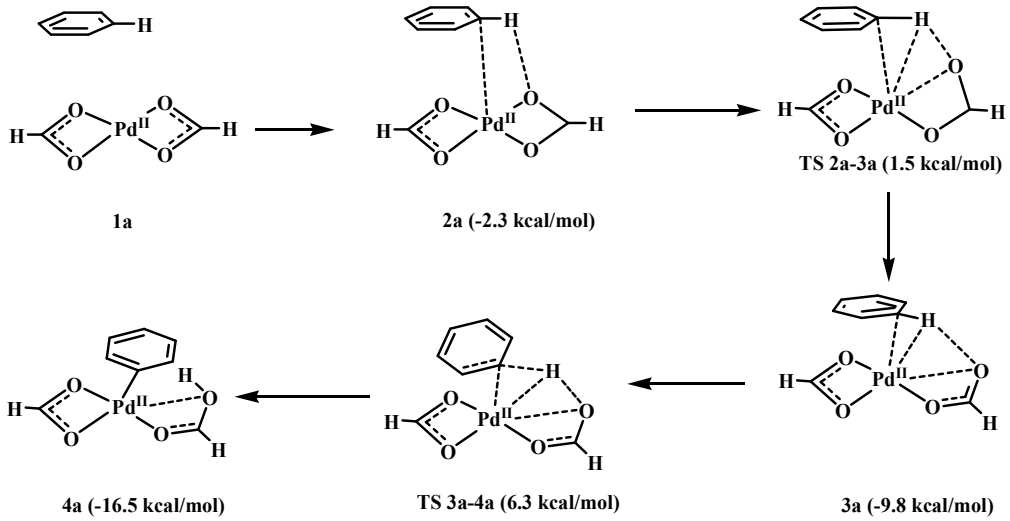

Scheme 7: C-H bond activation by benzene by $Pd(OOCH)_2$ and relative of energy of all the intermediates

Davies and Macgregor[12] demonstrate that in the presence of NaOAc, $[IrCl_2Cp^*]_2$ (Cp^* = η-C_5Me_5) react with N, N-dimethylbenzylamine and 2-phenyl-4,4-dimethyloxazoline to form a cyclometallated molecule (Scheme 8), in which the metal activates the phenyl ring. Moreover, the $[RhCl_2Cp^*]_2$ and $[RuCl_2(p\text{-cymene})]_2$cyclometallated with sodium acetate when an imine and a N-alkyl imine were present, respectively. The proton in this process can be abstracted by the acetate, which functions as a base.

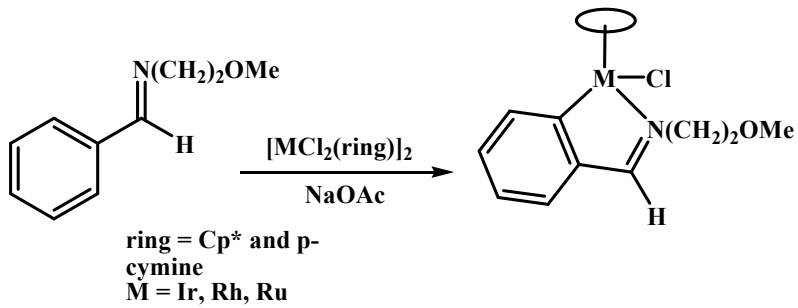

Scheme 8: Ir, Ru and Rh Cyclometallated compound

The mechanism of dimethylbenzyl amine (DMBA-H) and palladium-promoted C-H bond activation was calculated using the DFT method by Davies and Macgregor[13] (Scheme 9). Following the formation of the intermediate **1b**, oxygen leaves the metal

palladium through the transition state **TS 1b-2b,** the activation barrier in this case is 13 kcal/mol. The ultimate product, **3b**, is obtained by proton abstraction by acetate through a six-membered transition state, with an activation barrier of only 0.1 kcal/mol **TS 2b-3b**.

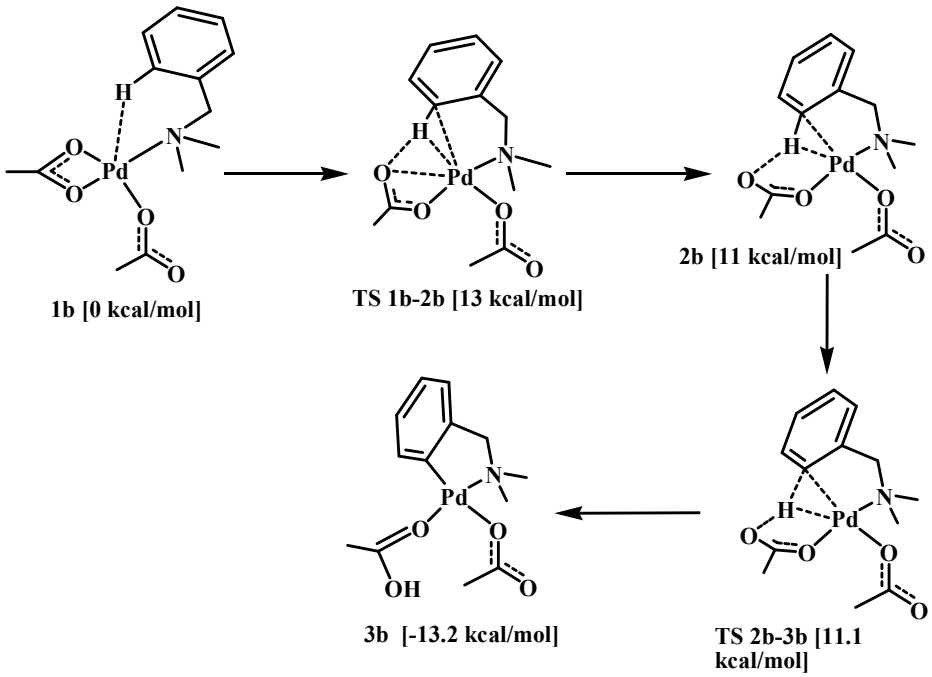

Scheme 9: Mechanism of acetate assisted C-H bond activation and relative energy of all the intermediates and transition states

Davies and Macgregor[14] performed the theoretical computation of the iridium metal complex {[Ir(DMBA-H)(κ^1-OAc)Cp]$^+$} (DMBA = N, N, dimethyl benzyl amine) (Scheme 10). Nitrogen-coordinated iridium intermediate **1c** was formed. Both electrophilic pathways I and II may be followed, it was observed. The electrophilic route I form **2c** by passing through the six-membered transition state **TS 1c-2c**, the activation barrier in this case is 16 kcal/mol. However, in electrophilic pathway II, the metal-bound oxygen can remove the proton from the phenyl ring through a four-membered transition state; after all, the activation barrier is 22.8 kcal/mol **TS 4c-5c**, and product **5c** is ultimately formed.

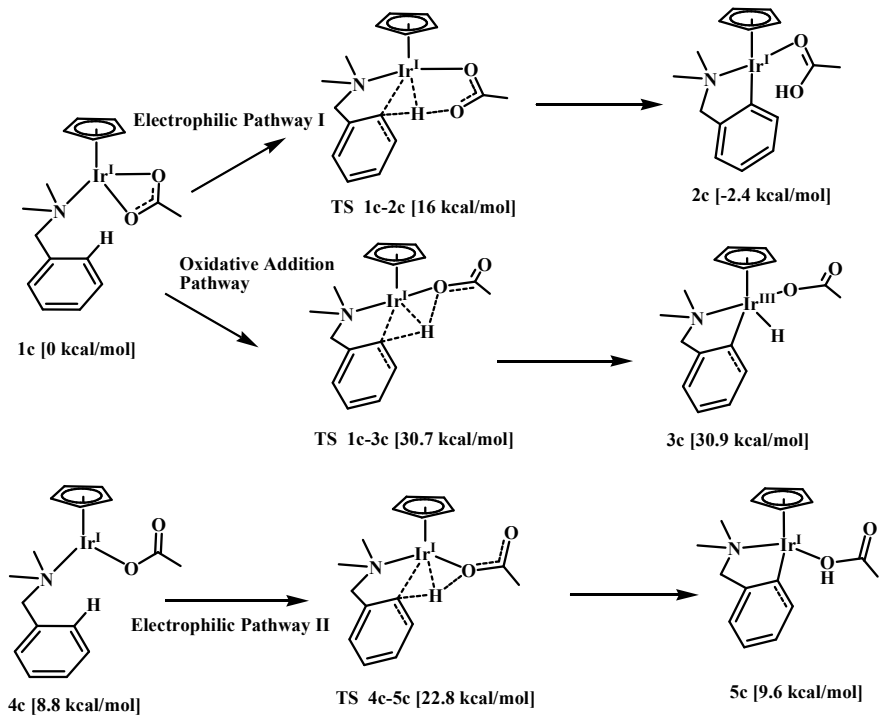

Scheme 10: C-H bond activation of $[Ir(DMBA-H)(OAc)Cp]^+$ and relative energy of all the intermediates and transition states

The oxidative addition pathway was also examined. In this case, the iridium hydride intermediate **3c** is formed through **TS 1c-3c** when phenyl hydrogen is oxidatively added to the **1c** intermediate. With an activation energy of 30.7 kcal/mol, it is significantly higher than other pathways. It was determined that, among the three paths, Pathway I (CMD) was the most advantageous.

The C-H bond activation of the nitrile-containing organic substrate was performed by Houk[15]*et al.* utilizing trimeric $Pd_3(OAc)_6$, dimeric $Pd_2(OAc)_4$, and heterodimeric $PdAg(OAc)_3$. The activation of the C-H bond will be the only topic covered here. $Pd(OAc)_2$ monomers and nitrile-containing substrates were used to study various C-H bond activation mechanisms. According to Scheme 11, the activation barrier for the oxidative addition process is 62.8 kcal/mol. The CMD process has an activation barrier of only 29.6 kcal/mol, the σ-bond metathesis path has an energy value of 48.3 kcal/mol, and the transition state of electrophilic aromatic substitution (**EAS**) reaction was not found. Based on these energy values, it was determined that the CMD path is more advantageous than the others.

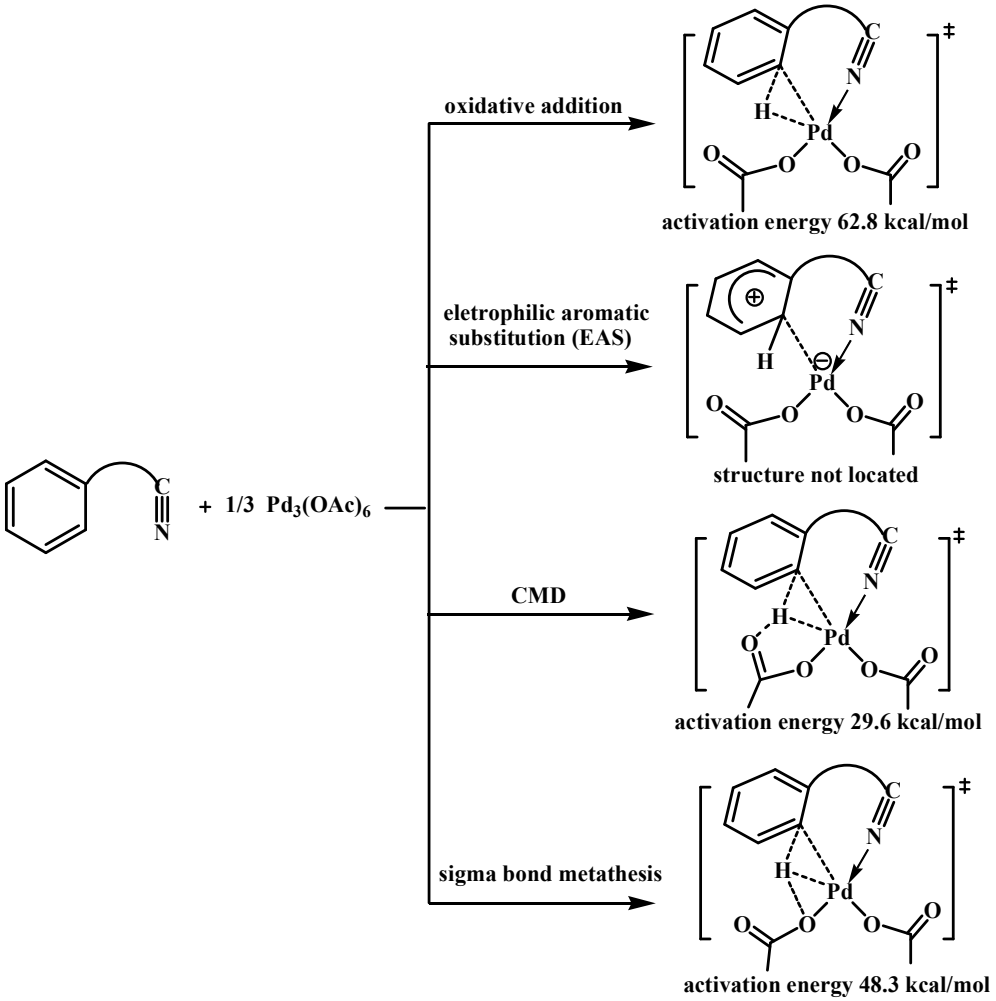

Scheme 11: C-H bond activation and computed activation energy

The entire process of C-H bond activation was now covered. Trimeric palladium acetate was first separated into monometallic palladium, which then interacted with a template nitrile-containing organic substrate to generate the nitrogen-coordinated intermediate **1d** (Scheme 12). Subsequently, one oxygen left the metal and phenyl hydrogen approached the acetate (intermediate **3d**). The intermediate **4d** can then be formed by acetate abstracting a proton from phenyl through transition state **TS 3d-4d**, the activation barrier is 29.6 kcal/mol.

For the dimeric $Pd_2(OAc)_4$, the same C-H bond activation mechanism was investigated (Scheme 13). First, the intermediate **2e** is formed; next, one oxygen separates from the metal; and finally, the phenyl carbon approaches the palladium

metal (intermediate **3e**). Through the transition state **TS 3e-4e**, the proton abstraction by one acetate results in the formation of intermediate **4e**. The activation barrier of this step is 19.4 kcal/mol.

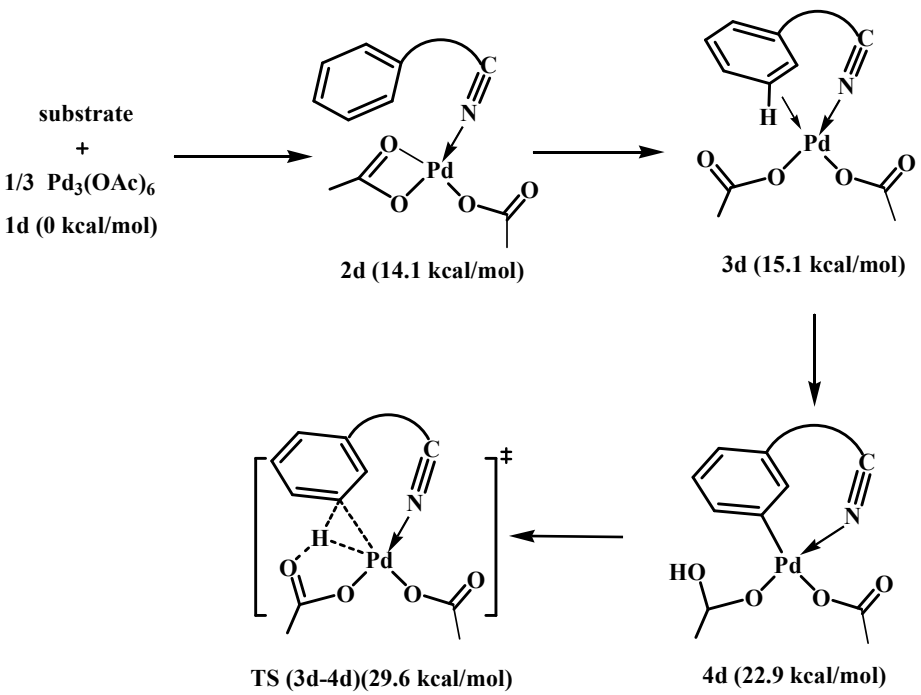

Scheme 12: C-H bond activation of nitrile containing template using species trimeric $Pd_3(OAc)_6$

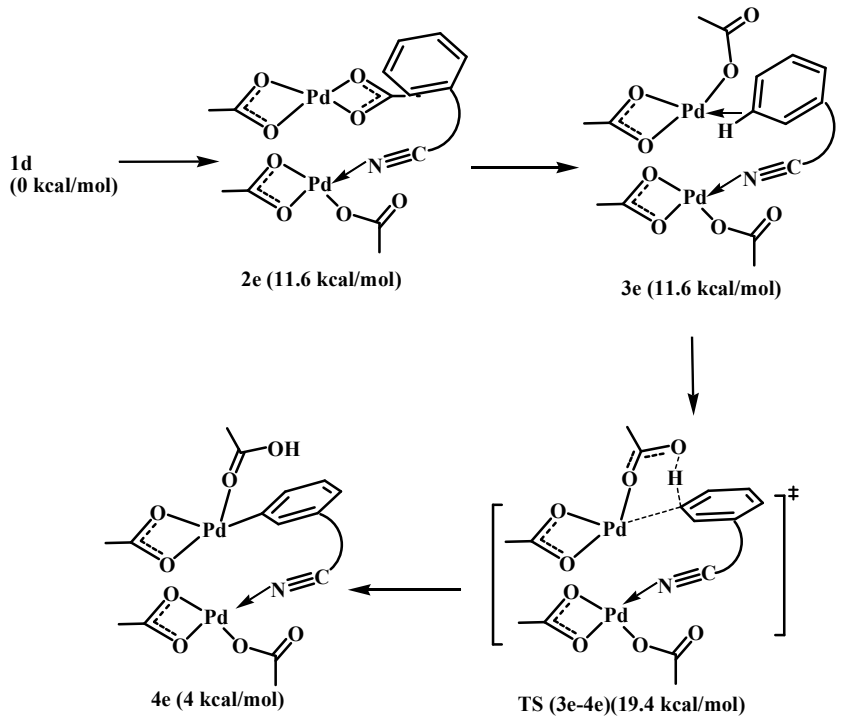

Scheme 13: C-H bond activation of nitrile containing template using species dimeric $Pd_2(OAc)_4$

When the same mechanistic details were used to take heterodimeric $PdAg(OAc)_3$, it was shown that the activation barrier for proton abstraction by acetate is only 11.2 kcal/mol (**TS 3f-4f)**, which is a lower energy barrier than the others (Scheme 14).

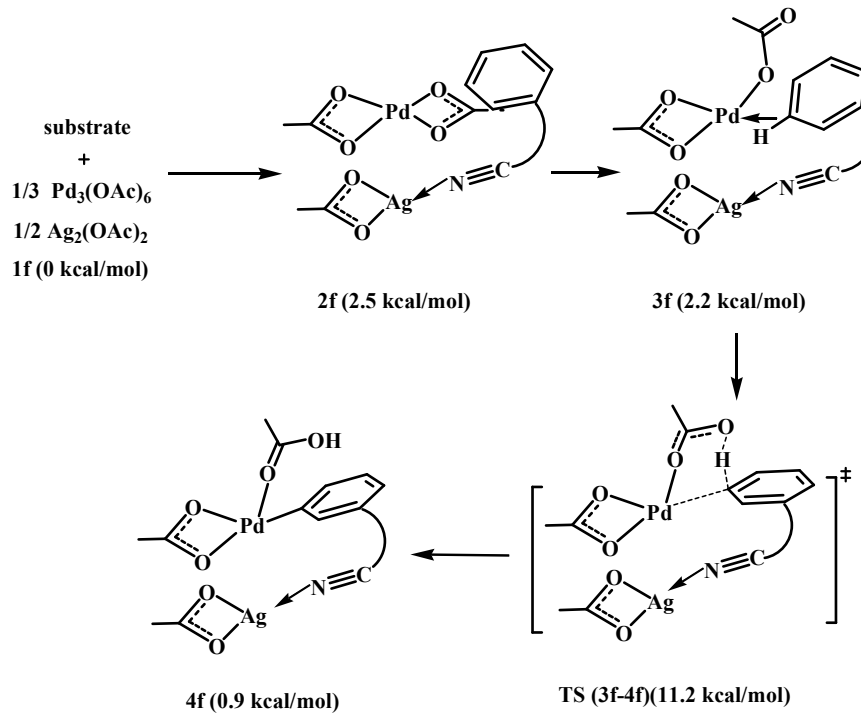

Scheme 14: C-H bond activation of nitrile containing template using species heterodimeric $PdAg(OAc)_3$

Catalytic C-H functionalization:

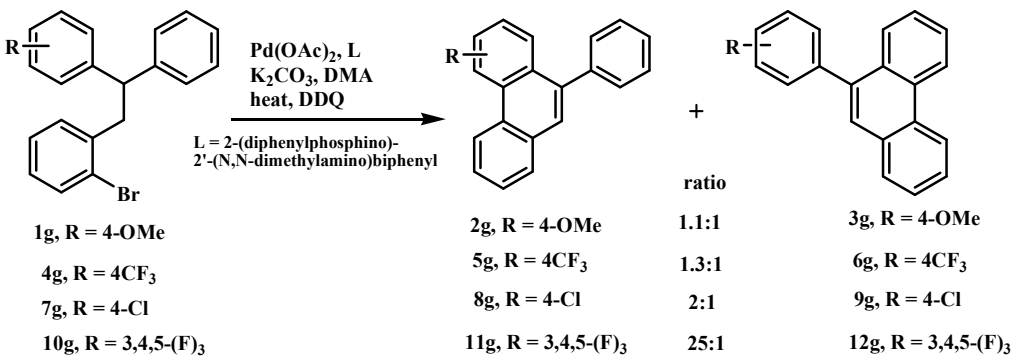

Scheme 15: Palladium catalysed arylation of organic compound

Echavarren[16] and Fagnou have contributed significantly to the field of palladium-catalyzed intramolecular arylation through their numerous publications. The intramolecular reaction of an aryl substrate with a $Pd(OAc)_2$ catalyst and **L** (Scheme 15) results in the formation of substituted phenanthrenes with regioisomeric ratios. The regioselective ratio for the electron-releasing group (OMe) is 1.1:1, whereas the

ratio range for the electron-withdrawing group (CF_3, Cl) is 1.3-2:1, indicating that it follows S_EAr processes. However, the trifluorophenyl produces only one product (ratio = 25:1), suggesting that it breaks the S_EAr process.In this reaction mixture the

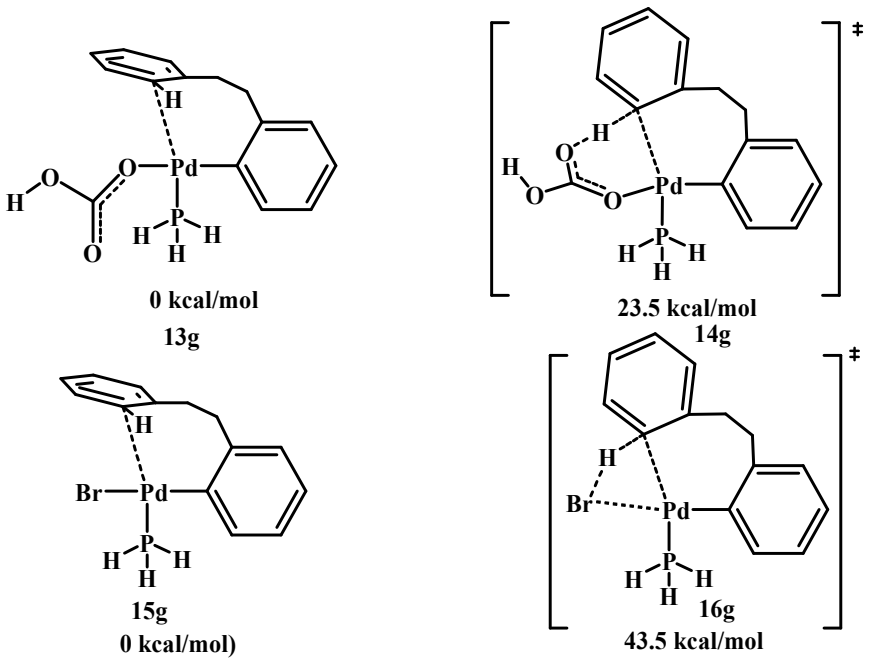

Figure 2: Carbonate, Bromide assited C-H bond activation of Palladium complex and computed energy of intermediates and transition state

K_2CO_3 was used as a base.

The mechanistic details were examined using DFT calculations. To do this, a **13g** intermediate was used as the starting material (Figure 2). In the transition state (**14g**), the proton of the phenyl ring was taken by HCO_3^-, and the carbon of the phenyl ring approached the metal atom and the activation barrier was 23.5 kcal/mol. The study was conducted using a trifluro phenyl ring, resulting in an activation barrier of only 13.2 kcal/mol. The same mechanism was applied to the bromide ion, resulting in a high activation energy of 43.5 kcal/mol in the transition state (**16g**), due to its weaker base compared to carbonate.

Using a palladium catalyst, Fagnou[17] also performed similar chemistry and found that the reaction between 3-fluorobenzothiophene (**7h**) and benzothiophene (**6h**) produced only a **9h** product (Scheme 16). Both the CMD mechanism and the kinetic data demonstrated that it does not follow the $S_EAr$mechanism. The activation energy

of arene substrates was calculated and shown in Figure 3, where H^a represents the activation energy of the experimental reacting side value.

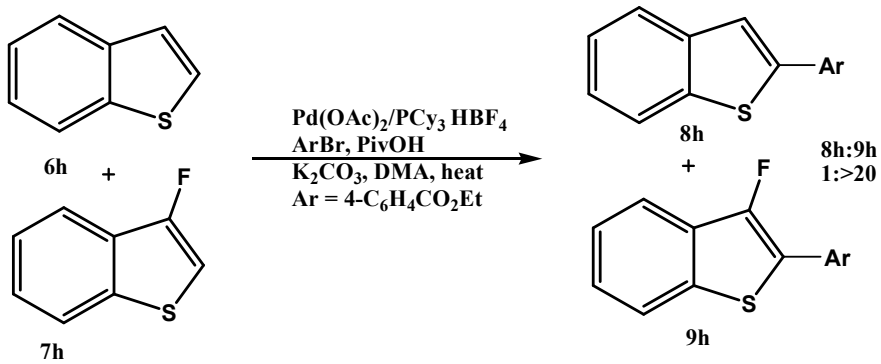

Scheme 16: Palladium Catalysed Arylation Reaction

The activation strain analysis (Scheme 17) was conducted to comprehend the regioselectivity of the reaction (8h:9h = 1:>20). Distortion energy is the energy required to distort **A** and **B** to transition state geometry **C** and **D**, while electronic interaction energy is the energy gained when **C** and **D** form transition state **E**. Data table 1 shows that π-electron-rich arenes **2h** and **3h** benefit from the largest negative E_{int} values, but large E_{dist} penalties cancel out this gain. Large E_{int} values, however, are not advantageous for electron-deficient (**4h**) arenes (Table 1).

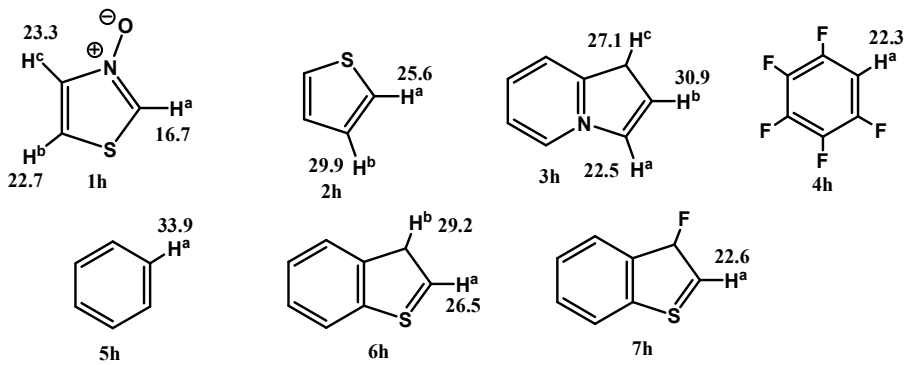

Figure 3: Computed free energy activation (kcal/mol) for arylation via CMD pathway, [a]experimental reaction site

Table 1: For the lowest free energy CMD state, Distortion/Interaction analysis

Arene	$\Delta E^{\#}$	E_{dist}(ArH)	E_{dist}(PdL)[a]	E_{int}
1h	5.8	29.3	16.6	-40.1
2h	15.9	39.9	17.4	-41.4
3h	13.1	48.1	19.9	-54.9
4h	11.9	28.8	15.3	-32.2
5h	25.1	44.6	15.8	-35.3
6h	16.7	37.5	16.8	-37.6
7h	12.3	32.4	17.2	-37.3

[a]Pd(Ph)(PMe_3)(OAc)

However, a more straightforward arene distortion results in a favourably low E_{dist}, which keeps the TS accessible. Thiazole N-oxides (**1h**) experience a small E_{dist} penalty and a large E_{int} gain. The benzene (**5h**) case exhibits unfavorable values, resulting in the highest $\Delta E^{‡}$ value among all arene (Table 1). This finding also explains why **7h** is more reactive than **6h**, the fluorine atom has minimal effect on E_{int} but causes a noticeable drop in E_{dist}, which makes arene palladation easier.

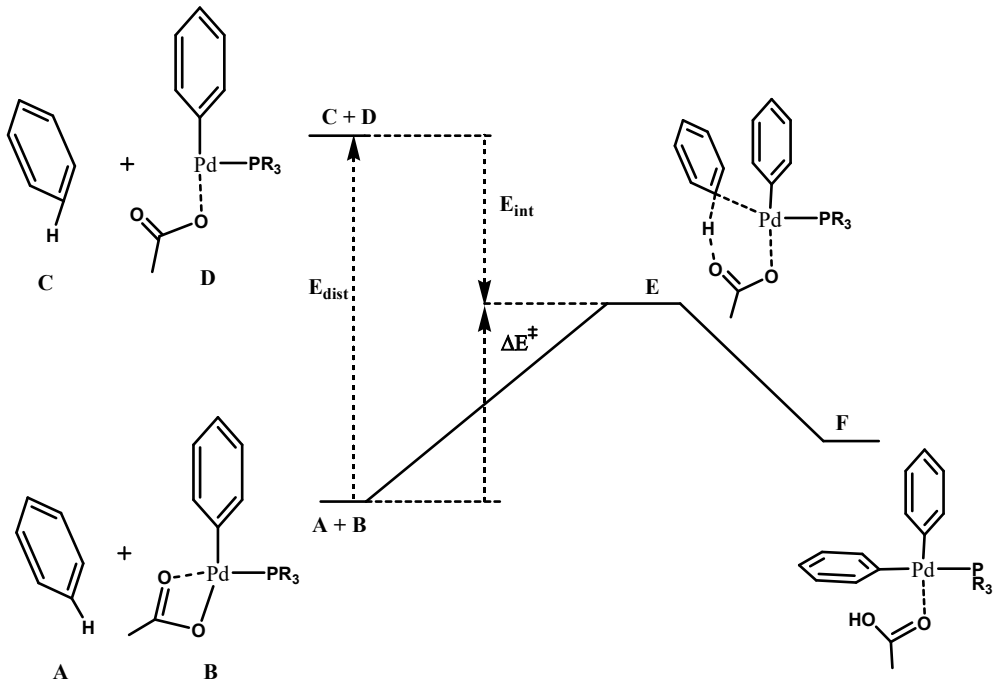

Scheme 17: Activation-Strain analysis

ELECTROPHILIC CONCERTED METALATION-DEPROTON (eCMD)[18]

Using electron-rich (2-methyl thiophene) and electron-deficient (C_6F_5H) substrates in a catalytic experiment with catalyst **5i** resulted in an exclusively electron-rich biaryl product (1i); in contrast, catalyst **8i** produced an exclusively electro-deficient biaryl product (4i) (Scheme 18). DFT calculations (Scheme 19) revealed that catalyst **5i** undergoes a transition state of **6i** when it reacts with an electron-rich substrate; the activation barrier is 19.6 kcal/mol. However, when an electron-poor substrate is reacted, it produces a transition state (**7i**) with an activation energy of 27.6 kcal/mol, indicating that the activation barrier is lower (8 kcal/mol) for the electron-rich substrate than for the electron-poor substrate. The opposite result was found when the same calculation was performed with catalyst **8i**; the activation barrier is lower (3.7 kcal/mol) for electron-poor substrates than for electron-rich substrates, which supports the experimental result (Scheme 18).

eCMD experiment

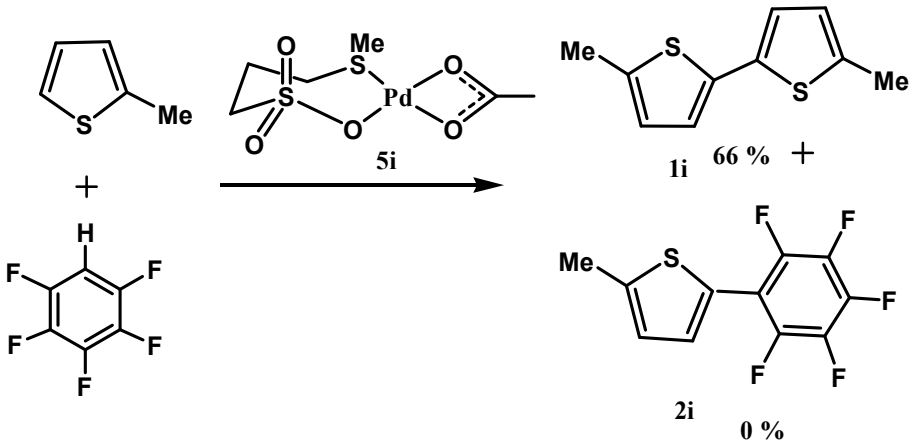

Standard CMD experiment

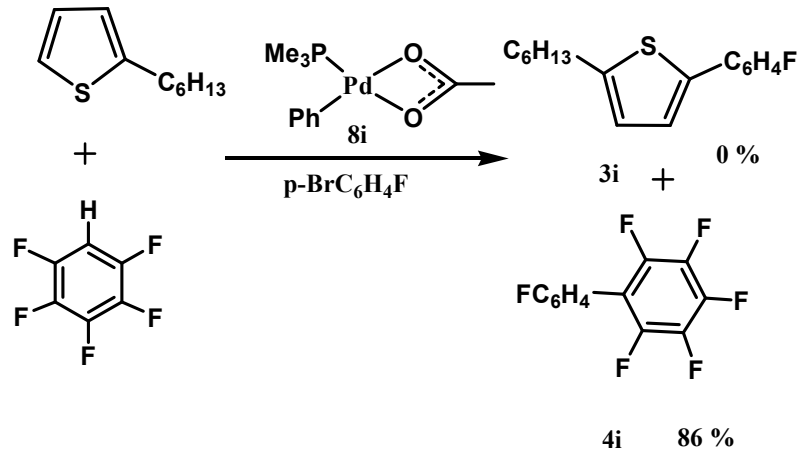

Scheme 18: Selectivity of catalytic reaction by an electrophilic Pd(II) complex (5i) or less electrophilic organo-Pd(II) complex (8i)

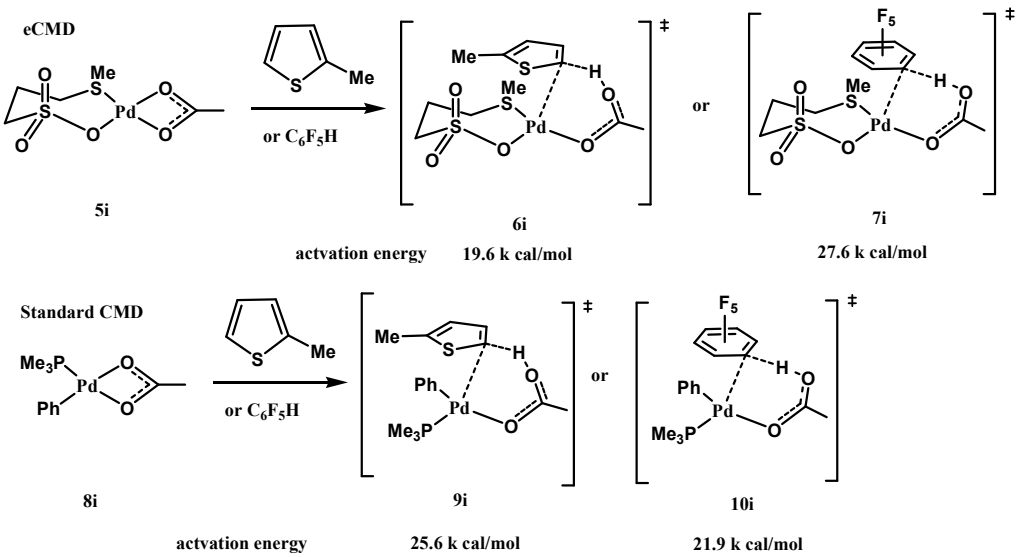

Scheme 19: Calculated activation energies for C-H bond activation in an electron rich (2-Methylthiophene) or electron poor (C_6F_5H) by an electrophilic Pd(II) {5i} complex or less electrophilic organo-Pd(II) complex {8i}

During the transition state of C-H bond activation, a nucleophilic catalyst (i. e., d^8 organometallic or d^{10} metal complexes) creates a partial negative charge in a substrate; this happens through the CMD mechanism (Figure 4). This reaction has a lower activation barrier because of polarity matching between the catalyst and electron-poor (hetero)arenes. In contrast with regular CMD, the electrophilic CMD (eCMD) process is the opposite of polarization in that the catalyst is more electrophilic (i. e., d^6 or d^8 complexes with weak X-type ligands) and the substrate is more electron-rich (Figure 4). Therefore, a number of parameters, including the catalyst's oxidation state, d-electron count, formal charge, and auxiliary ligands, distinguish ordinary CMD from eCMD.

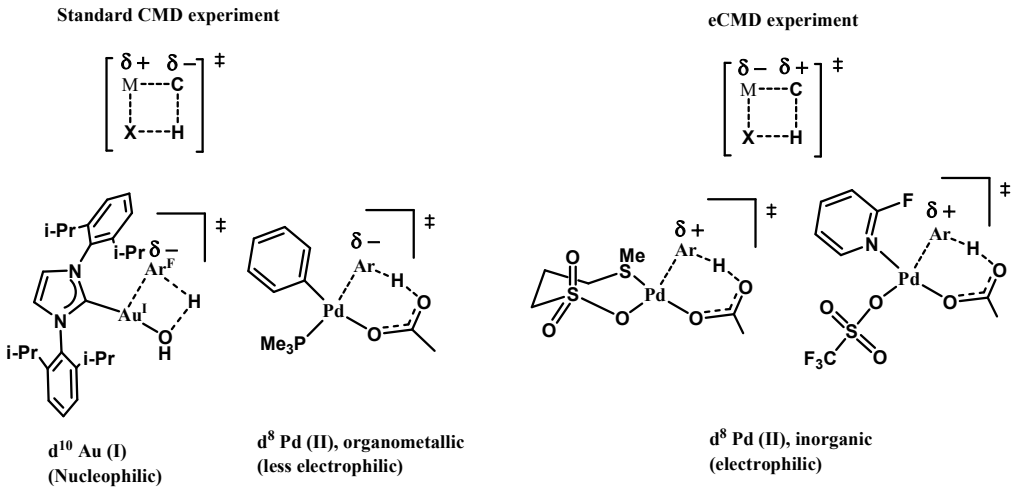

Figure 4: Metal catalyst used in standard CMD experiment and eCMD experiment

SUMMARY

This paper examined various C-H bond activation processes, with a particular focus on the mechanism of the CMD process. From the start, the evolution of cyclometallation reaction was covered. Cyclometallation compounds with transition metals including palladium, iridium, and rhodium were described with the right ligand design. It was addressed how the C-H bond activation process works mechanistically. Base-assisted C-H bond activation was found to be more advantageous than other C-H bond activation methods. Metal complexes governed the selectivity of C-H bond functionalization of electron-rich and electron-poor substrates; more electrophilic metal complexes favoured electron-rich C-H functionalization products, or electrophilic CMDs, while less electrophilic metal complexes favoured electron-poor C-H functionalization products, or standard CMDs.

Many studies on CMD are published each year, and it is hoped that it will be used in a variety of fields in the future, such as biology and chemistry.

REFERENCES

1. (a) *Handbook of C-H Transformation*, ed. by G. Dyker, Wiley-Interscience, New York, 2005. DOI: 10.1002/9783527619450
   (b) *Topics in Current Chemistry: C-H Activation*, ed. by J.-Q. Yu, Z. Shi, Springer, Berlin, 2010, Vol. 292.DOI:10.1007/978-3-642-12356-6
2. (a) Z. Y. Lin, *Coord. Chem. Rev.,* 2007, 251, 2280. https://doi.org/10.1016/j.ccr.2006.11.006 (b) Y. Boutadla, D. L. Davies, S. A. Macgregor, A. I. Poblador-Bahamonde, *Dalton Trans.* 2009, 5820. https://doi.org/10.1039/B904967C (c) D. Balcells, E. Clot, O. Eisenstein, *Chem. Rev.,* 2010, 110, 749.https://doi.org/10.1021/cr900315k
3. (a) D. L. Davies, S. A. Macgregor, C. L. McMullin, *Chem. Rev.* 2017, 117, 13, 8649. https://doi.org/10.1021/acs.chemrev.6b00839 (b) R. A. Alharis, C. L. McMullin, D. L. Davies, K. Singh, and S. A. Macgregor, *J. Am. Chem. Soc.,* 2019, 141, 22, 8896.https://doi.org/10.1021/jacs.9b02073 (c) N. Tamosiunaite, L. C. Logie, S. E. Neale, K. Singh, D. L. Davies, and S. A. Macgregor, *J. Org. Chem*, 2022, 87, 2, 1445. https://doi.org/10.1021/acs.joc.1c02756 (d) K. M. Altus, J. A. Love, *Commun Chem*, 2021, 173. https://doi.org/10.1038/s42004-021-00611-1 (e) V. Gandon and C. Hoarau, *J. Org. Chem.,* 2021, 86, 2, 1769. https://doi.org/10.1021/acs.joc.0c02604
4. Otto Dimroth (1902). "Ueber die MercurirungaromatischerVerbindungen". Berichte der deutschenchemischen Gesellschaft. 35 (2): 2032–2045. doi:10.1002/cber.190203502154
5. S. Winstein, T. G. Traylor, *J. Am. Chem. Soc.*, 1955, 77, 3747. https://doi.org/10.1021/ja01619a021
6. G. A. Olah, S. H. Yu, D. G. Parker, *J. Org. Chem.*, 1976, 41, 1983. https://doi.org/10.1021/jo00873a020
7. A. C. Cope, R. W. Siekman, *J. Am. Chem. Soc.,* 1965, 87, 3272 https://doi.org/10.1021/ja01092a063
8. A. C. Cope, E. C. Friedrich, *J. Am. Chem. Soc.*, 1968, 90, 909 https://doi.org/10.1021/ja01006a012
9. J. M. Davidson, C. Triggs, *J. Chem. Soc. A*, 1968, 1324. https://doi.org/10.1039/J19680001324
10. A. D. Ryabov, I. K. Sakodinskaya, A. K. Yatsimirsky, *J. Chem. Soc., Dalton Trans.*, 1985, 2629. https://doi.org/10.1039/DT9850002629
11. B. Biswas, M. Sugimoto, S. Sakak, Organometallics 2000, 19, 3895. https://doi.org/10.1021/om000002s
12. D. L. Davies, O. Al-Duaij, J. Fawcett, M. Giardiello, S. T. Hilton, D. R. Russell, *Dalton Trans.*, 2003, 4132. https://doi.org/10.1039/B303737A
13. D. L. Davies, S. M. A. Donald, S. A. Macgregor, *J. Am.Chem. Soc.,* 2005, 127, 13754. https://doi.org/10.1021/ja052047w
14. D. L. Davies, S. M. A. Donald, O. Al-Duaij, S. A. Macgregor, M. Pölleth, *J. Am. Chem. Soc.*, 2006, 128, 13, 4210. https://doi.org/10.1021/ja060173
15. Y. Yang, G. Cheng, P. Liu, D. Leow, T. Sun, P. Chen, X. Zhang, J. Yu, Y. Wu, K. N. Houk, *J. Am. Chem. Soc.*, 2014, 136, 1, 344. https://doi.org/10.1021/ja410485g
16. (a) D. García-Cuadrado, A. A. C. Braga, F. Maseras, A. M. Echavarren, *J. Am. Chem. Soc.*, 2006, 128, 4, 1066. https://doi.org/10.1021/ja056165v
    (b) J. J. González, N. García, B. Gómez-Lor, A. M. Echavarren, *J. Org. Chem.,* 1997, 62, 5, 1286. https://doi.org/10.1021/jo962059n

17. (a) S. I. Gorelsky, D. Lapointe, K. Fagnou, *J. Am. Chem. Soc.* 2008, 130, 33, 10848. https://doi.org/10.1021/ja802533u (b) S. I. Gorelsky, D. Lapointe, K. Fagnou, *J. Org. Chem.*, 2012, 77, 1, 658. https://doi.org/10.1021/jo202342q (c) L. Campeau, M. Parisien, M. Leblanc, K. Fagnou, *J. Am. Chem. Soc.*, 2004, 126, 30, 9186. https://doi.org/10.1021/ja049017y (d) M. Lafrance, N. Blaquière, K. Fagnou, *Chem. Commun.*, 2004, 2874. https://doi.org/10.1039/B410394G
18. (a) B. P. Carrow, J. Sampson, L. Wang, *Isr. J. Chem.*, 2020, 230. https://doi.org/10.1002/ijch.201900095 (b) L. Wang, B. P. Carrow, *ACS Catal.* 2019, 6821. https://doi.org/10.1021/acscatal.9b01195